atmosphere

MDPI

Article

Abundance of NO_3 Derived Organo-Nitrates and Their Importance in the Atmosphere

Amy Foulds [1,2,3], M. Anwar H. Khan [1,*], Thomas J. Bannan [3], Carl J. Percival [4], Mark H. Lowenberg [2] and Dudley E. Shallcross [1,5,*]

1 School of Chemistry, University of Bristol, Bristol BS8 1TS, UK; amy.foulds@manchester.ac.uk
2 Department of Aerospace Engineering, Queen's Building, University of Bristol, Bristol BS8 1TR, UK; m.lowenberg@bristol.ac.uk
3 The School of Earth, Atmospheric and Environmental Science, The University of Manchester, Oxford Road, Manchester M13 9PL, UK; Thomas.bannan@manchester.ac.uk
4 NASA Jet Propulsion Laboratory, California Institute of Technology, 4800 Oak Grove Dr, Pasadena, CA 91109, USA; carl.j.percival@jpl.nasa.gov
5 Department of Chemistry, University of the Western Cape, Robert Sobukwe Road, Bellville, Cape Town 7375, South Africa
* Correspondence: anwar.khan@bristol.ac.uk (M.A.H.K.); d.e.shallcross@bristol.ac.uk (D.E.S.); Tel.: +44-117-3317042 (M.A.H.K.); +44-117-9287796 (D.E.S.)

Abstract: The chemistry of the nitrate radical and its contribution to organo-nitrate formation in the troposphere has been investigated using a mesoscale 3-D chemistry and transport model, WRF-Chem-CRI. The model-measurement comparisons of NO_2, ozone and night-time N_2O_5 mixing ratios show good agreement supporting the model's ability to represent nitrate (NO_3) chemistry reasonably. Thirty-nine organo-nitrates in the model are formed exclusively either from the reaction of RO_2 with NO or by the reaction of NO_3 with alkenes. Temporal analysis highlighted a significant contribution of NO_3-derived organo-nitrates, even during daylight hours. Night-time NO_3-derived organo-nitrates were found to be 3-fold higher than that in the daytime. The reactivity of daytime NO_3 could be more competitive than previously thought, with losses due to reaction with VOCs (and subsequent organo-nitrate formation) likely to be just as important as photolysis. This has highlighted the significance of NO_3 in daytime organo-nitrate formation, with potential implications for air quality, climate and human health. Estimated atmospheric lifetimes of organo-nitrates showed that the organo-nitrates act as NO_x reservoirs, with particularly short-lived species impacting on air quality as contributors to downwind ozone formation.

Keywords: organo-nitrates; atmospheric lifetime; ozone; secondary organic aerosol; air quality

Citation: Foulds, A.; Khan, M.A.H.; Bannan, T.J.; Percival, C.J.; Lowenberg, M.H.; Shallcross, D.E. Abundance of NO_3 Derived Organo-Nitrates and Their Importance in the Atmosphere. *Atmosphere* **2021**, *12*, 1381. https://doi.org/10.3390/atmos12111381

Academic Editor: Rafael Borge

Received: 5 September 2021
Accepted: 20 October 2021
Published: 22 October 2021

1. Introduction

The nitrate radical (NO_3) dominates night-time oxidation in urban areas in particular, where NO_2 and O_3 levels are elevated [1–4]. However, many studies have also highlighted the significance of NO_3 in oxidation chemistry over extensive regions of the atmosphere, with high concentrations being reported over a range of atmospheric conditions [1,5,6] and a suggestion that the highest levels exist in the residual boundary layer [7].

Generated from the relatively slow oxidation of NO_2 by O_3 (Reaction (1)), NO_3 only exists in significant concentrations during the night, reaching mixing ratios of 1 ppt or less in remote regions and 10–400 ppt in polluted urban regions [8–12]. Rapid photolysis rates and efficient reaction with NO result in suppressing NO_3 mixing ratios with lifetimes of approximately 5 s [13] during daytime hours, but elevated levels have been predicted in winter for example [3,4].

$$NO_2 + O_3 \rightarrow NO_3 + O_2 \quad (1)$$

NO_3 can react with NO_2 to establish a thermal equilibrium with nitrogen pentoxide (N_2O_5) on a timescale of minutes in the boundary layer (Reaction (2)).

$$NO_2 + NO_3 + M \leftrightharpoons N_2O_5 + M \quad (2)$$

The NO_3 radical has a significant impact on atmospheric composition at night-time due to its reaction with numerous unsaturated hydrocarbons [14], thereby influencing the budgets of these species and their degradation products. The reactions of NO_3 with unsaturated hydrocarbons, both biogenic and anthropogenic, lead to the formation of multifunctional organo-nitrates [15–17].

Organo-nitrates ($RONO_2$) are mainly formed in the atmosphere through photochemical and nocturnal oxidation of anthropogenic and biogenic volatile organic compounds (VOCs); this process is initiated by the OH and NO_3 radicals, respectively [18]. During the day, peroxy radicals (RO_2) are mainly produced via reaction of VOCs with the OH radical, Cl radical and ozone. These radicals then go on to react with NO by two different pathways: one leads to NO-to-NO_2 conversion and hence produces ozone (Reactions (3)–(5)) and the other produces organo-nitrates (Reaction (6)). The branching ratios of Reaction (6) are highly variable with the chain length of the alkyl group, e.g., $\leq$1% for $C_2H_5ONO_2$ and ~33% for n-$C_8H_{17}ONO_2$ [19]. During the night, the formation of organo-nitrates is dominated by NO_3. It is highly reactive towards unsaturated hydrocarbons [14,20], adding to the double bond and generating organo-nitrates via this route (Reaction (7)).

$$RO_2 + NO \rightarrow RO + NO_2 \quad (3)$$

$$NO_2 + h\nu \rightarrow NO + O(^3P) \quad (4)$$

$$O(^3P) + O_2 + M \rightarrow O_3 + M\ (M{=}N_2{,}O_2) \quad (5)$$

$$RO_2 + NO \rightarrow RONO_2 \quad (6)$$

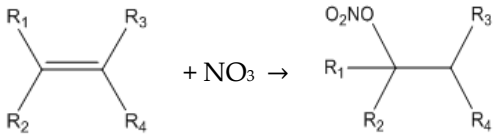

(7)

Organic nitrate destruction occurs via photolysis and reaction with OH.

$$RONO_2 + h\nu \rightarrow RO + NO_2 \quad (8)$$

$$RONO_2 + OH \rightarrow \text{Products} \quad (9)$$

The relative importance of these two destruction pathways depends on the net UV light intensity, the size of the nitrate and the substitution pattern [21]. For the alkyl nitrates with shorter chain length ($\leq$C4), photolysis is the dominant loss process, whereas for the alkyl nitrates with longer carbon chain ($\geq$C4), oxidation by OH is the dominant loss process [22–24]. The alkyl nitrates act as NO_x reservoirs, releasing their sequestered NO_x by these destruction processes (Reactionss (8) and (9)), which can contribute to photochemical production of O_3 in areas far remote from NO_x sources.

Organo-nitrates can contribute to regional ozone formation and subsequently affect air quality [25–30]. Several studies highlight the formation of organo-nitrates through the reaction of NO_3 and unsaturated hydrocarbons such as isoprene and monoterpenes, which have low vapor pressures, allowing them to condense to generate a significant amount of SOA [18,31–35]. A study by Ng et al. [36] reported an SOA yield of between approximately 4 and 24% (in terms of organic mass) when considering the reaction between isoprene and NO_3, thus highlighting the significance of these species as SOA precursors. These aerosols are known to have a major impact on the climate and human health [37–42].

The complexity of nitrate chemistry and the associated atmospheric and epidemiological implications due to the formation of organo-nitrates drive the need for continued research into the atmospheric processes, which govern NO_3 and organo-nitrates in general. An important aspect of this research is the assessment of how models represent nitrate chemistry, as these are useful tools for simulating the processes governing the composition of the atmosphere during both the day- and night-time hours. We used a regional air quality model, WRF-Chem-CRI, to investigate the nitrate chemistry by comparing the model N_2O_5, NO_2 and ozone mixing ratios with measured N_2O_5, NO_2 and ozone mixing ratios collected during the summer months of the ClearfLo project [43], along with the processes which govern organo-nitrate formation.

2. Methodology

2.1. Measurement Site and Measurement Technique

There were no measurements of NO_3 during the ClearfLo campaign; instead, we used measured N_2O_5, NO_2 and ozone to compare modelled N_2O_5, NO_2 and ozone, which provide an indication of the model's ability to represent nitrate chemistry, particularly in terms of NO_3. The measurements were made at an urban background site in North Kensington during the summer of the ClearfLo project using a CIMS instrument for N_2O_5, a chemiluminescence instrument (Air Quality Inc., Oregon City, OR, USA) for NO_2 and a UV absorption TEI 49C and 49i (Thermo Scientific, Waltham, MA, USA) for ozone. The details of the instrument and the inlet configuration are described elsewhere [44,45]. The site is located within the grounds of Sion Manning School at 51.521055° N, 0.213432° W. The school is situated within a residential area approximately 7 km west of central London. The road is in close proximity to the site (10 m away) and is a minor road that only experiences high traffic volumes during school drop-off and pick-up times and rush-hour periods. There is also a major road approximately 100 m from the site, which experiences sustained high traffic volumes over the course of the day. The instrument inlet on-site was deployed at a height of ~4 m from the ground.

The N_2O_5 measurement was performed using a quadrupole chemical ionisation mass spectrometer (CIMS) using iodide ions (I) to detect N_2O_5 as NO_3^- (m/z = 62) at a frequency of 1 Hz. Calibration and backgrounding procedures are presented in Bannan et al. [46]. Studies such as Wang et al. [47] have noted that measurements of N_2O_5 at m/z 62 are not interference-free, with HNO_3 and HO_2NO_2 being identified as key species that could cause interferences at this m/z. Measurements of N_2O_5 are now routinely made at m/z 235 with iodide CIMS. Nevertheless, Le Breton et al. [48] and Bannan et al. [46] measured N_2O_5 at m/z 62 concurrently with the Broadband Cavity Enhanced Absorption Spectrometer (BBCEAS) on both ground and airborne measurement campaigns where very good agreement was seen, albeit in more remote locations. Measurements presented here are therefore upper limits of night-time N_2O_5 as interferences in this measurement location are more likely in comparison to previously reported inter-comparison studies with this instrument.

2.2. WRF-Chem-CRI Model

WRF-Chem-CRI is a regional-scale, three-dimensional meteorological model with online chemistry. The model is fully coupled, whereby the chemistry and aerosol components along with the prognostic meteorological parameters are integrated over the same timestep as the transport processes, using the same advection and physical parameterisations [49]. Meteorological boundary conditions were taken from the European Centre for Medium-Range Forecasts (ECMWF) ERA-Interim reanalysis data [50]. The Model for Ozone And Related chemical Tracers (MOZART) model is an offline global transport model [51] that is used to account for the long-range transport of chemical species from outside the model domain. Biogenic emissions were estimated using an online canopy-scale model, the Model of Emissions of Gases and Aerosols from Nature (MEGAN) [52,53]. The anthropogenic emission for the UK is used in WRF-Chem-CRI from the National Atmospheric Emissions Inventory (NAEI), with a resolution of 1 km by 1 km (http://naei.beis.gov.uk;

accessed on 30 September 2021). A coarser emissions database is used for Europe, e.g., TNO emission inventory [54], with a resolution of 0.125° longitude by 0.0625° latitude. The gas-phase scheme used in this study was a reduced chemical scheme, CRI-MECH, which was developed using the Master Chemical Mechanism version 3.1 (MCM 3.1), reducing the number of species and reactions by 90%, with ozone production by a given species equivalent to the number of NO to NO_2 conversions that take place during its complete degradation being the primary criterion [55,56]. The CRI-MECH scheme contains 229 species, 529 gas-phase reactions and 96 photolytic reactions. The rate coefficients for the reactions in CRI-MECH specified as a function of temperature were taken from either the MCM (http://mcm.york.ac.uk/; accessed on 30 September 2021) and/or the Jet Propulsion Laboratory kinetic evaluation reports (http://jpldataeval.jpl.nasa.gov/, accessed on 30 September 2021). The model calculates photolysis using the Fast-J scheme [57] and links it to the chemical mechanism in the model. Photolysis rates in and below clouds are modulated by the Fast-J scheme using the aerosol population extinction and phase function to account for the influence of clouds and aerosols. A domain was run using a horizontal grid spacing of 15 km and a size of 134 (E-W) by 146 (N-S) grid points, covering the UK and NW Europe using a Lambert conformal map projection [58,59]. The simulation was run from 00:00 UTC on 30 July 2012 to 00:00 UTC 18 August 2012. The meteorological field was re-initialized every 3 days to ensure that the divergence of the WRF-Chem-CRI meteorology from the driving ECMWF operational/reanalysis meteorology is minimized.

3. Results and Discussion

3.1. Model Validation

The model performance of NO_3 has been examined by comparing the model-measurements of NO_2, O_3 and N_2O_5 mixing ratios because of their strong dependency on the steady-state concentration of NO_3. As shown in the midday and midnight ozone data, the trends in the model predictions are generally very similar to the observations (Figure 1). The modelled O_3 data have strong correlations with measurements, having the coefficient of determination (r^2) of 0.84 and 0.57 for midday and midnight, respectively. The difference between modelled and measured ozone data referred to as 'bias' are found to be −1.4 ppb for midday and −3.4 ppb for midnight. The modelled under-predictions of ozone in North Kensington are most notable at night, which could be due to the capping of the boundary layer in the model being too strong, preventing the replenishment of ground-level ozone with that from the free troposphere. The predicted midday and midnight NO_2 data also show similar trends to the observations (Figure 1), with a reasonable correlation (r^2 = 0.29 for midday and 0.34 for midnight) and a reasonable bias (−4.5 ppb for midday and −0.4 ppb for midnight). The model underestimation of NO_2 is found to be higher during daytime compared with night-time, which can be explained by the coarse resolution of WRF-Chem-CRI, meaning that the processing of sub-grid scale emissions and fast NO_x photochemistry is not captured in the simulations, thus acting as a source of model uncertainty. The measured data of N_2O_5 are only for night-time, which is considered as an upper-limit measurement. We compared the modelled and the measured night-time N_2O_5 at the surface level and found a similar trend (Figure 1) with a good correlation (r^2 = 0.52), but with a sustained underestimation of model N_2O_5 mixing ratios (bias = −116 ppt). The model did not apply surface dynamics, assuming a uniform, flat surface, thus resulting in an underestimation of the model surface night-time N_2O_5 levels. The upper limits of measured night-time N_2O_5 because of the interferences in this urban background location are more likely responsible for the large disagreement between model-measurement of N_2O_5. A recent study [60] showed that HNO_3 would account for >70% of the signal at m/z = 62. Considering this interference in the measurement data of N_2O_5 could reduce the bias to −16 ppt (~85%). Overall, the WRF-Chem-CRI model performs well in terms of predicting, NO_2, O_3, and night-time N_2O_5 levels at the North Kensington site during the ClearfLo project. Therefore, it can be assumed that the NO_3 in the model provides a reasonable representation of levels present in the atmosphere.

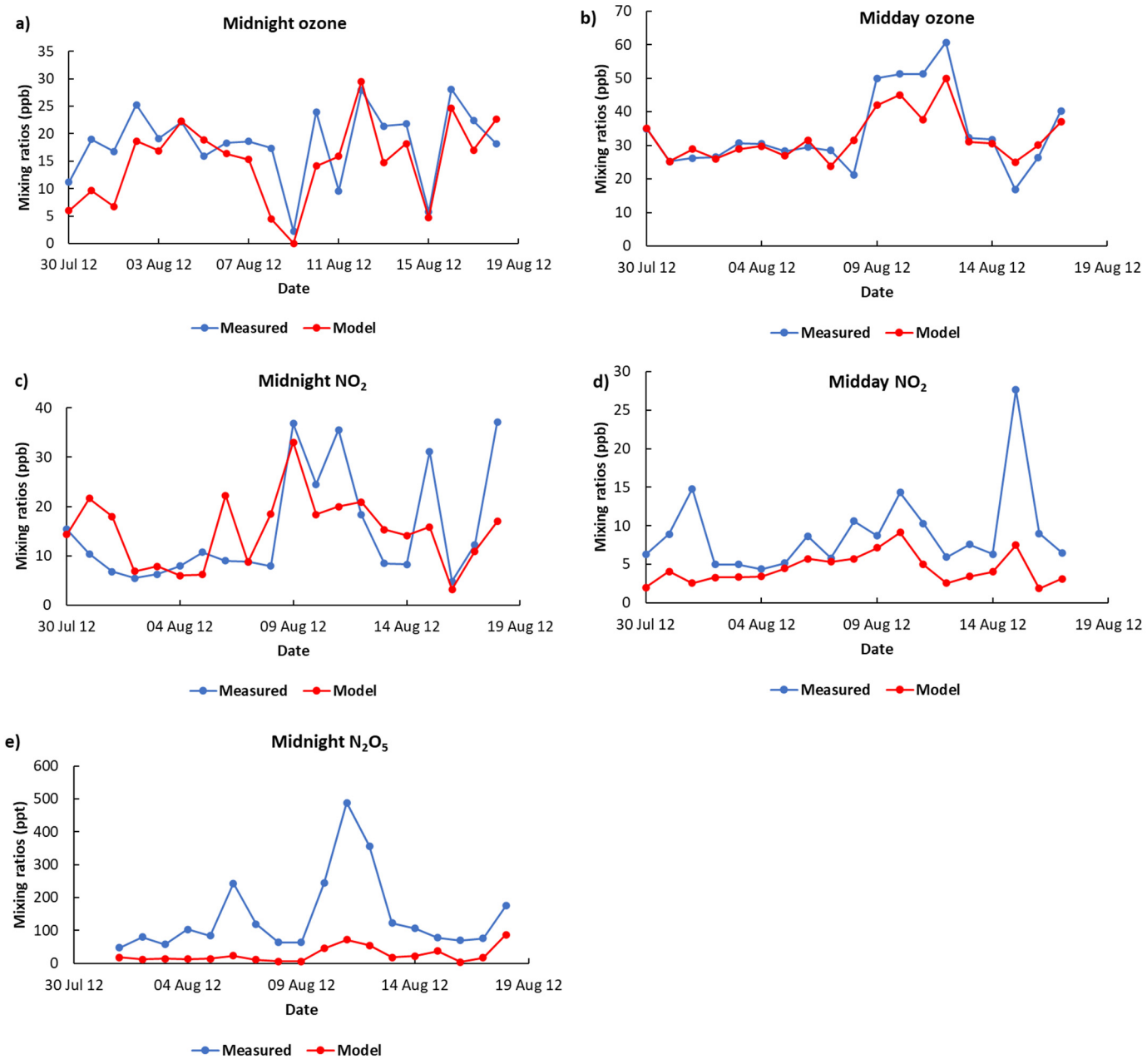

Figure 1. Comparison of (**a**) midnight ozone, (**b**) midday ozone, (**c**) midnight NO_2, (**d**) midday NO_2 and (**e**) midnight N_2O_5 mixing ratios modelled by WRF-Chem-CRI with those measured during the summer months of the ClearfLo project.

3.2. Contribution of NO_3 Sources Organo-Nitrates

We investigated the formation of 39 organo-nitrates in WRF-Chem-CRI from the production pathways (Table 1) and found that the organo-nitrates are formed solely from the reaction of RO_2 with NO (61%) and the reaction of NO_3 with alkenes (39%). Modelled mixing ratios of all 39 organo-nitrates from midnight and midday were extracted for each day for the urban background site in North Kensington, which were used for the calculation of the proportion of organo-nitrates formed from NO_3. The modelled organo-nitrate mixing ratio for midday (118 ± 103 ppt) is found to be ~2-fold higher than that for midnight (71 ± 47 ppt).

Table 1. Organo-nitrate species (shown in CRI names) and their respective production pathways and precursors, as represented in the CRI-v2 mechanism of WRF-Chem-CRI.

Organo-Nitrate Species *	Production Pathway
CH3NO3 (CH3NO3)	CH3O2 + NO
C2H5NO3 (C2H5NO3)	C2H5O2 + NO
IC3H7NO3 (IC3H7NO3)	IC3H7O2 + NO
HOC2H4NO3 (HOC2H4NO3)	HOCH2CH2O2+ NO
NRU12O2 (C510O2, NC4CO3)	C5H8 + NO_3
NRU12OOH (C510OOH, NC4CO3H)	C5H8 + NO_3
NRN6O2 (ETHENO3O2)	C2H4 + NO_3
NRN6OOH (ETHO2HNO3)	C2H4 + NO_3
NRN9O2 (PRONO3AO2, PRONO3BO2)	C3H6 + NO_3
NRN9OOH (PR1O2HNO3, PR2O2HNO3)	C3H6 + NO_3
NRN12O2 (C42NO33O2)	TBUT2ENE + NO_3
NRN12OOH (C42NO33OOH)	TBUT2ENE + NO_3
NOA (NOA)	C5H8 + NO_3
RN10NO3 (NC3H7NO3)	RN10O2 (NC3H7O2) + NO
RN13NO3 (NC4H9NO3, SC4H9NO3)	RN13O2 (NC4H9O2, SC4H9O2) + NO
RN19NO3 (HEXCNO3, M2PEDNO3, M3PECNO3)	RN19O2 (HEXCO2, M2PEDO2, M3PECO2) + NO
RN9NO3 (PROPOLNO3, PROLNO3)	RN9O2 (HYPROPO2, IPROPOLO2) + NO
RN12NO3 (HO1C4NO3, BUT2OLNO3)	RN12O2 (HO1C4O2, BUT2OLO2) + NO
RN15NO3 (PE1ENEANO3, PE2ENEANO3, HO2C5NO3)	RN15O2 (PE1ENEAO2, PE2ENEAO2, HO2C5O2) + NO
RN18NO3 (C65OH4NO3, C6OH5NO3, HO2C6NO3)	RN18O2 (C65OH4O2, C6OH5O2, HO2C6O2) + NO
RN16NO3 (PEANO3, PEBNO3, PECNO3)	RN16O2 (PEAO2, PEBO2, PECO2) + NO
RU14NO3 (ISOPANO3, ISOPBNO3, ISOPCNO3, ISOPDNO3)	RU14O2 (ISOPAO2, ISOPBO2, ISOPCO2, ISOPDO2) + NO
RA13NO3 (BZBIPERNO3)	RA13O2 (BZBIPERO2) + NO
RA16NO3 (TLBIPERNO3)	RA16O2 (TLBIPERO2) + NO
RA19NO3 (OXYBIPENO3)	RA19AO2 (OXYBIPERO2) + NO
RA25NO3 (DM35EBNO3)	RA25O2 (DM35EBO2) + NO
RA22NO3 (TM123BNO3)	RA22AO2 (TM123BO2) + NO
RTN28NO3 (APINANO3, APINBNO3, APINCNO3)	RTN28O2 (APINAO2, APINBO2, APINCO2) + NO
NRTN28O2 (NAPINAO2, NAPINBO2)	APINENE + NO_3
NRTN28OOH (NAPINAOOH, NAPINBOOH)	APINENE + NO_3
RTN25NO3 (C96NO3)	RTN25O2 (C96O2) + NO
RTN23NO3 (C98NO3)	RTN23O2 (C98O2) + NO
RTX24NO3 (NOPINANO3, NOPINBNO3, NOPINCNO3)	RTX24O2 (NOPINAO2, NOPINBO2, NOPINCO2) + NO
RTX22NO3 (C915NO3, C917NO3, C918NO3)	RTX22O2 (C915O2, C917O2, C918O2) + NO
RTX28NO3 (BPINANO3, BPINBNO3, BPINCNO3)	RTX28O2 (BPINAO2, BPINBO2, BPINCO2) + NO
NRTX28O2 (NBPINAO2, NBPINBO2)	BPINENE + NO_3
NRTX28OOH (NBPINAOOH, NBPINBOOH)	BPINENE + NO_3
NRU14O2 (NISOPO2)	C5H8 + NO_3
NRU14OOH (NISOPOOH)	C5H8 + NO_3

Note: MCM v3.3.1 analogues of the species are shown in parentheses. * Structures can be obtained using species name and search facility on MCM website (http://mcm.leeds.ac.uk/MCM/; accessed on 30 September 2021).

The contribution of organo-nitrate formation shows that a significant fraction of organo-nitrates at the urban North Kensington site is produced from NO_3 in summer (see Figure 2). During summer months, the midnight NO_3-sourced organo-nitrate (~62%) is found to be 3-fold higher than that at midday (~21%), which can be explained by the lower abundances of NO_3 due to its strong photolysis and OH losses during midday. However, there are still substantial contributions to organo-nitrate formation through VOCs + NO_3 during daytime for summer months suggesting that the reaction with VOCs in the environment with high levels of VOCs can significantly contribute to the loss of NO_3. Previous studies have reported similar findings with regard to the reactivity of NO_3, with losses of NO_3 from reactions with organic trace gases being large enough to compete with its photolysis and reaction with NO [3,61,62]. These findings highlight the fact that the NO_3 radical could be having a more dominant role in daytime oxidation than previously thought.

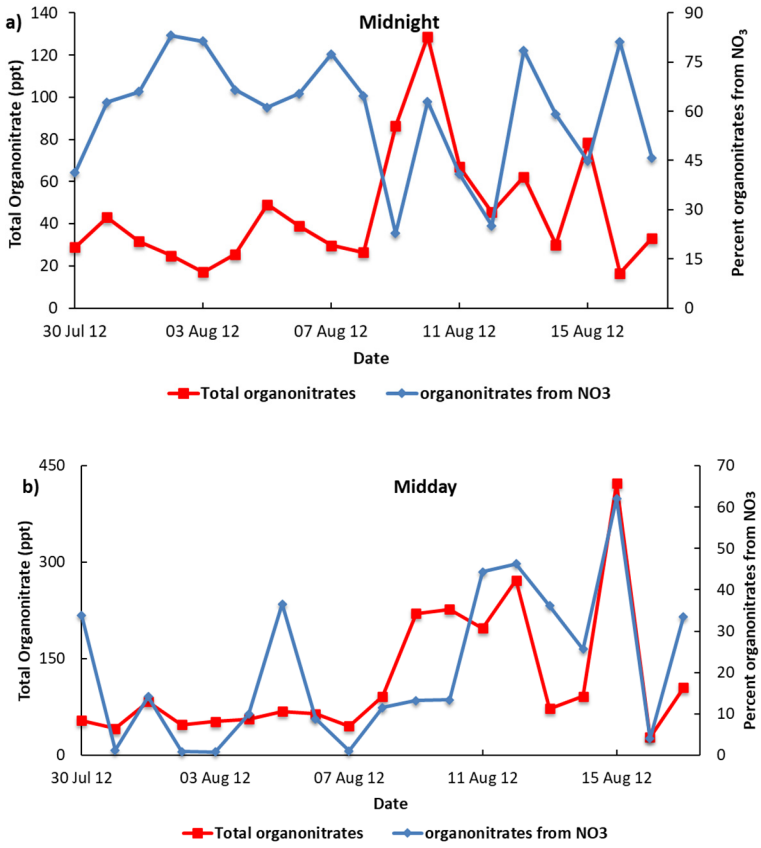

Figure 2. Total organo-nitrate and contributions sourced from NO_3 (**a**) midnight and (**b**) midday in North Kensington during summer months.

3.3. Atmospheric Implications of NO_3-Sourced Organo-Nitrates

The impacts of the organo-nitrates on the atmosphere, both in terms of SOA formation and their potential contribution to O_3 formation, are governed by their lifetimes, i.e., how quickly they degrade within the atmosphere. Thus, the lifetimes of these NO_3-derived organo-nitrates were estimated in order to gain insight into their implications for air quality.

The eight longest-lived organo-nitrates derived from NO_3 in the WRF-Chem-CRI model are: NRU12OOH (MCM analogues: C510OOH, NC4CO3H), NRN6OOH (MCM analogue: ETHO2HNO3), NRN9OOH (MCM analogues: PR1O2HNO3, PR2O2HNO3), NRN12OOH (MCM analogue: C42NO33OOH), NRTN28OOH (MCM analogues: NAPINAOOH, NAPINBOOH), NOA (MCM analogue: NOA), NRTX28OOH (MCM analogues: NBPINAOOH, NBPINBOOH) and NRU14OOH (MCM analogue: NISOPOOH).

In the model, each of these eight organo-nitrates is either lost by photolysis or by reaction with the OH radical, and the deposition loss of these organo-nitrates is not considered because of their low Henry's law constants [63]. Model fluxes associated with these reactions, along with global modelled concentrations, were used to derive estimated lifetimes for each organo-nitrate with respect to each loss process. The lifetimes were calculated for the months of July and August. The losses of seven NO_3-sourced nitrates (except NOA) in WRF-Chem-CRI are controlled by reaction with the OH radical, with shorter lifetimes often seen in July and August months, due to higher OH abundances and photolysis rates (see Table 2). For example, NRN12OOH has a shorter lifetime of around 1.0 day in July and August months (Table 2). It is likely that these seven nitrates will act as short- or long-term NO_x reservoirs, thus having implications for O_3 formation and air quality in and around London urban areas. However, NOA is an exception to this, with photolysis dominating its atmospheric loss.

Table 2. The estimated atmospheric lifetimes of 8 selected organo-nitrates (derived from NO_3) with respect to OH and photolysis loss.

Organo-Nitrates	Lifetime (July–August) (Days)	
	OH	Photolysis
NRN12OOH	1.0	10.7
NRN9OOH	1.3	11.1
NRN6OOH	1.7	10.9
NRU12OOH	0.3	5.1
NRU14OOH	0.4	36.5
NRTN28OOH	0.8	9.0
NRTX28OOH	0.7	7.4
NOA	42.1	17.1

As highlighted previously, the lifetime of these species dictates the impact that they will have on surrounding air quality. For example, in the case of NOA, its lifetime stays relatively constant at approximately 16 days. Based on the assumption that it takes approximately 1 day for an air mass to cross the U.K., organo-nitrates with these longer lifetimes will act as long-term reservoirs of NO_x, persisting in the atmosphere and being essentially inert in terms of impacts on atmospheric composition or air quality in the U.K. However, the remaining seven are shorter-lived organo-nitrates, with lifetimes of less than 3 days and will start to have an impact locally, the extent of which will have a dependence on wind speed.

Two isoprene-derived organo-nitrates in WRF-Chem-CRI which are particularly short-lived are NRU12OOH and NRU14OOH. These only persist on a timescale of a few hours, thus making them short-term NO_x reservoirs with definite impacts on local and regional air quality. In order to understand the atmospheric implications of these organo-nitrates, one must consider their chemistry and the impacts associated with their degradation products. NRU12OOH reacts with the OH radical to produce another organo-nitrate, NOA, which in turn degrades to produce NO_2 and the acetyl peroxy radical ($CH_3C(O)O_2$). With a lifetime of between 6 and 7 h, an air mass containing NRU12OOH would have enough time to travel away from where it was generated. This means that this organo-nitrate would contribute to O_3 production downwind the following day (based on the assumption that it is predominantly generated during the night), thus acting as a potential source of O_3 downwind. NRU14OOH reacts with the OH radical to generate multigenerational organo-nitrates. This ultimately results in the formation of NOA, which decomposes to release NO_2. As with NRU12OOH, the lifetime of NRU14OOH (approximately 9 h) allows the air to travel away from where it was generated, thus contributing to O_3 formation downwind. However, its slightly longer lifetime and the less direct route of producing NOA means that NRU14OOH is able to transport the NO_x further from the source, thus contributing to O_3 formation and impacting air quality over a wider area.

To quantify the extent of ozone formation from organo-nitrates, another simulation was performed that involved WRF-Chem-CRI being integrated with the exclusion of the chemistry of organo-nitrates in CRI referred to as 'WRF-Chem-CRI-WON'. Comparing the ozone midday and midnight mixing ratios from WRF-Chem-CRI to WRF-Chem-CRI-WON in North Kensington during July-August shows that up to 1.5 ppb (4%) and 0.8 ppb (2.5%) ozone can be increased during daytime and night-time, respectively, suggesting that organo-nitrates can make a non-negligible contribution to the formation of O_3. During midday, the peaks of ozone increase are seen on 12 August 2012 (1.5 ppb; 4%) and 15 August 2012 (1.2 ppb; 3%) (Figure 3a) when the total organo-nitrates and NO_3-derived organo-nitrates are the highest among the whole data series (see Figure 2b). The trend of increase in ozone and NO_2 for midday is very similar (Pearson correlation, R = 0.7; Figure 3a,b), suggesting that the increase

in ozone downwind from North Kensington is associated with maximum NO_2 change (e.g., an episode of 12 August 2012; see Figure 4). The ozone increases during midnight are found to be high on 6–7 August 2012, 10–12 August and 14–15 August 2012; however, the ozone increases do not correlate very well (Pearson correlation, R = 0.3) with the increases of NO_2 (see Figure 3c,d). This suggests that the ozone formed from organo-nitrates are transported from Europe to North Kensington rather than locally formed (e.g., an episode of 11 August 2012; see Figure 4).

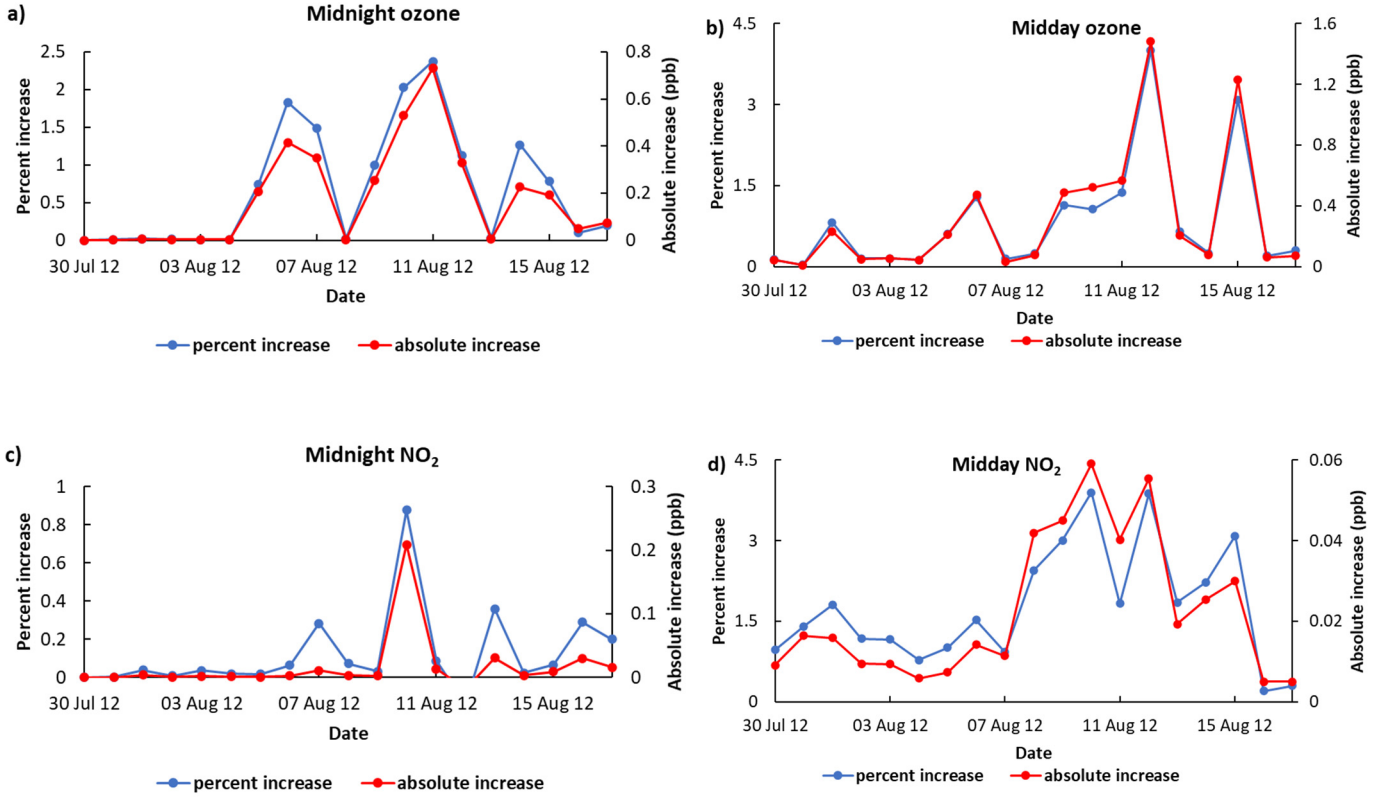

Figure 3. The percent and absolute increase in ozone and NO_2 from WRF-Chem-CRI to WRF-Chem-CRI-WON for (**a**) midnight ozone, (**b**) midday ozone, (**c**) midnight NO_2, (**d**) midday NO_2. Note: Absolute increase = (WRF-Chem-CRI–WRF-Chem-CRI-WON) and percent increase = (WRF-Chem-CRI–WRF-Chem-CRI-WON) × 100)/WRF-Chem-CRI-WON.

At present, the CRI (Common Representative Intermediates) mechanism traceable to the MCM (Master Chemical Mechanism) used in the WRF-Chem model does not contain organo-nitrates-derived SOA and is focused on optimising the representation of NO–NO_2 conversions rather than SOA formation. This consequently means that the model is currently underestimating the SOA contribution from organo-nitrates. The previous study showed that the organo-nitrates (e.g., RTX28NO3, RTN28NO3) in the global model, STOCHEM-CRI, have an impact on SOA formation with a non-negligible contribution (~5%) to the total simulated global SOA [64]. The model, STOCHEM-CRI output [65] shows 0.026 μg m^{-3} SOA formed from the organo-nitrates, which is ~20% of the total simulated SOA (0.16 μg m^{-3}) formed in the North Kensington in July–August. This therefore highlights the importance of organo-nitrates in the atmosphere and has scope for improving the representation of SOA in the WRF-Chem-CRI model, as the organo-nitrates represented in the chemical mechanism are likely to play an important role in this area.

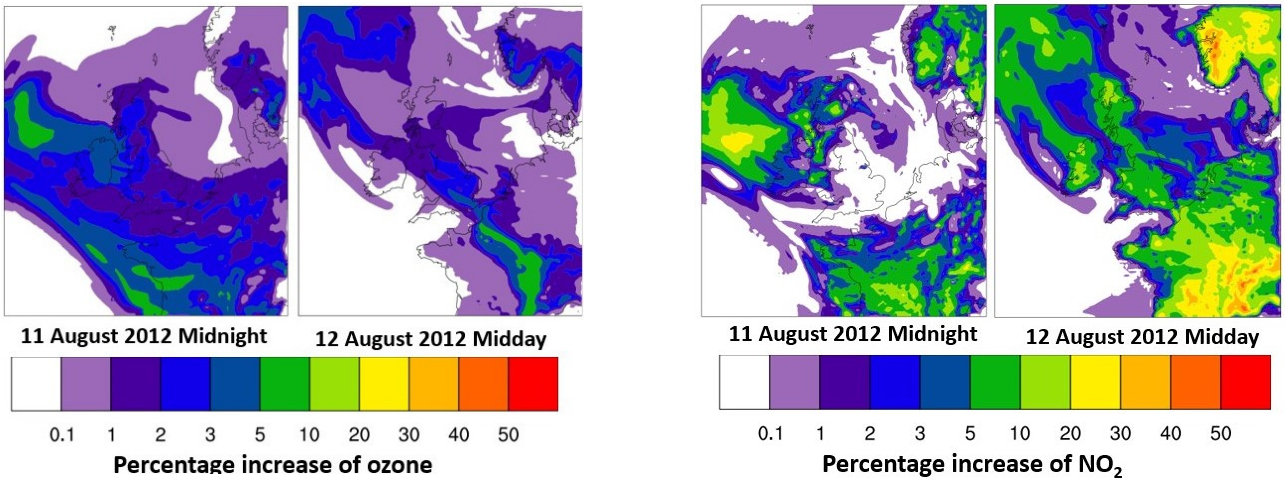

Figure 4. Percent increases of surface ozone and NO_2 mixing ratios from WRF-Chem-CRI to WRF-Chem-CRI-WON at 11 August 2012 midnight and 12 August 2012 midday. Note: Percent increase = (WRF-Chem-CRI–WRF-Chem-CRI-WON) × 100)/WRF-Chem-CRI-WON.

4. Conclusions

NO_3 has long been recognised as the dominant oxidising species in the night-time polluted troposphere, having a significant impact on the degradation chemistry and budgets of numerous VOCs. In the study, the measured night-time N_2O_5, NO_2 and ozone during the summer were used to assess the model's ability to represent nitrate chemistry (NO_3). Extraction of midday and midnight mixing ratios of organo-nitrates gave insight into how the fraction of NO_3-derived organo-nitrate varies according to time of day. The temporal and day-night analysis showed that a significant fraction of organo-nitrates are formed from NO_3, even during daylight hours, attesting to a more dominant role in daytime organo-nitrate formation than previously thought. The lifetimes of selected long-lived organo-nitrates with respect to the OH radical and photolysis were then estimated, with analysis finding that most organo-nitrates were dominated by OH oxidation. Lifetimes varied on a timescale of days, highlighting their roles as short- and long-term NO_x reservoirs and resultant implications for O_3 production, air quality and human health. Two isoprene-derived organo-nitrates in particular, NRU12OOH and NRU14OOH were found to persist on a timescale of hours, thus making them likely to contribute to O_3 formation and impact on local air quality. The analysis showed that the organo-nitrates can contribute ozone formation up to ~1.6 ppb (midday) and ~0.8 ppb (midnight) at North Kensington during the summer months. This analysis also showed that the organo-nitrates currently represented in WRF-Chem-CRI do not readily condense and therefore do not contribute to SOA. These results highlight the need to consider and improve the SOA representation in the model in the future.

Author Contributions: A.F. and M.A.H.K. analyzed the data and wrote the paper; D.E.S. conceived and designed the project; T.J.B. and C.J.P. performed the measurement of N_2O_5; C.J.P., M.H.L., T.J.B. and D.E.S. reviewed and edited the manuscript. All authors have read and agreed to the published version of the manuscript.

Funding: A.F. thanks EPSRC for her PhD studentship. M.A.H.K. and D.E.S. thank NERC (grant code-NE/K004905/1), Bristol ChemLabS and the Primary Science Teaching Trust under whose auspices various aspects of this work was supported. C.J.P.'s work was carried out at Jet Propulsion Laboratory, California Institute of Technology, under contract with the National Aeronautics and Space Administration (NASA), and was supported by the Upper Atmosphere Research and Tropospheric Chemistry Programs.

Institutional Review Board Statement: Not applicable.

Informed Consent Statement: Not applicable.

Data Availability Statement: The data presented in this study are available on request from the corresponding authors.

Acknowledgments: We thank Douglas Lowe for his continuous supports about WRF-Chem modelling throughout the project. We thank the three anonymous reviewers for their insightful reviews and suggestions which has benefitted this manuscript.

Conflicts of Interest: The authors declare no conflict of interest.

References

1. Wayne, R.P.; Barnes, I.; Biggs, P.; Burrows, J.P.; Canosas-Mas, C.E.; Hjorth, J.; Le Bras, G.; Moortgat, G.K.; Perner, D.; Poulet, G.; et al. The nitrate radical: Physics, chemistry, and the atmosphere. *Atmos. Environ.* **1991**, *25*, 1–203. [CrossRef]
2. Platt, U.; Alicke, B.; Dubois, R.; Geyer, A.; Hofzumahaus, A.; Holland, F.; Martinez, M.; Mihelcic, D.; Klüpfel, T.; Lohrmann, B.; et al. Free radicals and fast photochemistry during BERLIOZ. *J. Atmos. Chem.* **2002**, *42*, 359–394. [CrossRef]
3. Khan, M.A.H.; Morris, W.C.; Watson, L.A.; Galloway, M.; Hamer, P.D.; Shallcross, B.M.A.; Percival, C.J.; Shallcross, D.E. Estimation of daytime NO_3 radical levels in the UK urban atmosphere using the steady state approximation method. *Adv. Meteorol.* **2015**, *2015*, 294069. [CrossRef]
4. Khan, M.A.H.; Cooke, M.C.; Utembe, S.R.; Archibald, A.T.; Derwent, R.G.; Xiao, P.; Percival, C.J.; Jenkin, M.E.; Morris, W.C.; Shallcross, D.E. Global modelling of the nitrate radical (NO_3) for present and pre-industrial scenarios. *Atmos. Res.* **2015**, *164*, 347–357. [CrossRef]
5. Brown, S.S.; Stutz, J. Nighttime radical observations and chemistry. *Chem. Soc. Rev.* **2012**, *41*, 6405–6447. [CrossRef]
6. Brown, S.S.; Ryerson, T.B.; Wollny, A.G.; Brock, C.A.; Peltier, R.; Sullivan, A.P.; Weber, R.J.; Dubé, W.P.; Trainer, M.; Meagher, J.F.; et al. Variability in nocturnal nitrogen oxide processing and its role in regional air quality. *Science* **2006**, *311*, 67–70. [CrossRef] [PubMed]
7. Fish, D.J.; Shallcross, D.E.; Jones, R.L. The vertical distribution of NO_3 in the atmospheric boundary layer. *Atmos. Environ.* **1999**, *33*, 687–691. [CrossRef]
8. Stone, D.; Evans, M.J.; Walker, H.; Ingham, T.; Vaughan, S.; Ouyang, B.; Kennedy, O.J.; McLeod, M.W.; Jones, R.L.; Hopkins, J.; et al. Radical chemistry at night: Comparisons between observed and modelled HO_x, NO_3 and N_2O_5 during the RONOCO project. *Atmos. Chem. Phys.* **2014**, *14*, 1299–1321. [CrossRef]
9. Aliwell, S.R.; Jones, R.L. Measurements of tropospheric NO_3 at midaltitude. *J. Geophys. Res. Atmos.* **1998**, *103*, 5719–5727. [CrossRef]
10. Finlayson-Pitts, B.J.; Pitts, J.N., Jr. *Chemistry of the Upper and Lower Atmosphere: Theory, Experiments, and Applications*; Academic Press: Cambidge, MA, USA, 2000.
11. Asaf, D.; Tas, E.; Pedersen, D.; Peleg, M.; Luria, M. Long-Term Measurements of NO_3 Radical at a Semiarid Urban Site: 2. Seasonal Trends and Loss Mechanisms. *Environ. Sci. Technol.* **2010**, *44*, 5901–5907. [CrossRef] [PubMed]
12. Ng, N.L.; Brown, S.S.; Archibald, A.T.; Atlas, E.; Cohen, R.C.; Crowley, J.N.; Day, D.A.; Donahue, N.M.; Fry, J.L.; Fuchs, H.; et al. Nitrate radicals and biogenic volatile organic compounds: Oxidation, mechanisms, and organic aerosol. *Atmos. Chem. Phys.* **2017**, *17*, 2103–2162. [CrossRef] [PubMed]
13. Seinfeld, J.H.; Pandis, S.N. *Atmospheric Chemistry and Physics*; John Wiley and Sons: Hoboken, NJ, USA, 1998.
14. Atkinson, R. Kinetics and mechanism of the gas-phase reactions of the NO_3 radical with organic compounds. *J. Phys. Chem. Ref. Data* **1991**, *20*, 459–507. [CrossRef]
15. Platt, U.; LeBras, G.; Poulet, G.; Burrows, J.P.; Moortgat, G. Peroxy radicals from night-time reaction of NO_3 with organic compounds. *Nature* **1990**, *348*, 147–149. [CrossRef]
16. Geyer, A.; Alicke, B.; Ackermann, R.; Martinez, M.; Harder, H.; BRUNE, W.; di Carlo, P.; Williams, E.; Jobson, T.; Hall, S.; et al. Direct observations of daytime NO_3: Implications for urban boundary layer chemistry. *J. Geophys. Res. Atmos.* **2003**, *108*, 4368. [CrossRef]
17. Huang, W.; Saathoff, H.; Shen, X.; Ramisetty, R.; Leisner, T.; Mohr, C. Chemical Characterization of Highly Functionalized Organonitrates Contribution to Night-Time Organic Aerosol Mass Loadings and Particle Growth. *Environ. Sci. Technol.* **2019**, *53*, 1165–1174. [CrossRef] [PubMed]
18. Farmer, D.K.; Matsunaga, A.; Docherty, K.S.; Surratt, J.D.; Seinfeld, J.H.; Ziemann, P.J.; Jimenez, J.L. Response of an aerosol mass spectrometer to organonitrates and organosulfates and implications for atmospheric chemistry. *Proc. Natl. Acad. Sci. USA* **2010**, *107*, 6670–6675. [CrossRef]
19. Atkinson, R.; Aschmann, S.M.; Carter, W.P.; Winer, A.M.; Pitts, J.N., Jr. Alkyl nitrate formation from the nitrogen oxide (NO_x)-air photooxidations of C_2-C_8 n-alkanes. *J. Phys. Chem.* **1982**, *86*, 4563–4569. [CrossRef]
20. Geyer, A.; Ackermann, R.; Dubois, R.; Lohrmann, B.; Müller, R.; Platt, U. Long-term observation of nitrate radicals in the continental boundary layer near Berlin. *Atmos. Environ.* **2001**, *35*, 3619–3631. [CrossRef]
21. Roberts, J.M. The atmospheric chemistry of organic nitrates. *Atmos. Environ.* **1990**, *24*, 243–287. [CrossRef]

22. Clemitshaw, K.C.; Williams, J.; Rattigan, O.V.; Shallcross, D.E.; Law, K.S.; Cox, R.A. Gas-phase ultraviolet absorption cross-sections and atmospheric lifetimes of several C_2-C_5 alkyl nitrates. *J. Photoch. Photobio. A* **1997**, *102*, 117–126. [CrossRef]
23. Flocke, F.; Volz-Thomas, A.; Buers, H.J.; Patz, W.; Garthe, H.J.; Kley, D. Long-term measurements of alkyl nitrates in southern Germany: 1. General behavior and seasonal and diurnal variation. *J. Geophys. Res.* **1998**, *103*, 5729–5746. [CrossRef]
24. Talukdar, R.K.; Burkholder, J.B.; Hunter, M.; Gilles, M.K.; Roberts, J.M.; Ravishankara, A.R. Atmospheric fate of several alkyl nitrates Part 2 UV absorption cross-sections and photodissociation quantum yields. *J. Chem. Soc. Faraday Trans.* **1997**, *93*, 2797–2805. [CrossRef]
25. Von Kuhlmann, R.; Lawrence, M.G.; Pöschl, U.; Crutzen, P.J. Sensitivities in global scale modeling of isoprene. *Atmos. Chem. Phys.* **2004**, *4*, 1–17. [CrossRef]
26. Fiore, A.M.; Horowitz, L.W.; Purves, D.W.; Levy, H.; Evans, M.J.; Wang, Y.; Li, Q.; Yantosca, R.M. Evaluating the contributing of changes in isoprene emissions to surface ozone trends over the eastern United States. *J. Geophys. Res. Atmos.* **2005**, *110*, D12303. [CrossRef]
27. Horowitz, L.W.; Fiore, A.M.; Milly, G.P.; Cohen, R.C.; Perring, A.; Wooldridge, P.J.; Hess, P.G.; Emmons, L.K.; Lamarque, J.-F. Observational constraints on the chemistry of isoprene nitrates over the eastern United States. *J. Geophys. Res. Atmos.* **2007**, *112*, D12S08. [CrossRef]
28. Perring, A.E.; Bertram, T.H.; Farmer, D.K.; Wooldridge, P.J.; Dibb, J.; Blake, N.J.; Blake, D.R.; Singh, H.B.; Fuelberg, H.; Diskin, G.; et al. The production and persistence of $\Sigma RONO_2$ in the Mexico City plume. *Atmos. Chem. Phys.* **2010**, *10*, 7215–7229. [CrossRef]
29. Farmer, D.K.; Perring, A.E.; Wooldridge, P.J.; Blake, D.R.; Baker, A.; Meinardi, S.; Huey, L.G.; Tanner, D.; Vargas, O.; Cohen, R.C. Impact of organic nitrates on urban ozone production. *Atmos. Chem. Phys.* **2011**, *11*, 4085–4094. [CrossRef]
30. Paulot, F.; Henze, D.K.; Wennberg, P.O. Impact of the isoprene photochemical cascade on tropical ozone. *Atmos. Chem. Phys.* **2012**, *12*, 1307–1325. [CrossRef]
31. Griffin, R.J.; Cocker, D.R.; Flagan, R.C.; Seinfeld, J.H. Organic aerosol formation from the oxidation of biogenic hydrocarbons. *J. Geophys. Res. Atmos.* **1999**, *104*, 3555–3567. [CrossRef]
32. Lee, A.; Goldstein, A.H.; Kroll, J.H.; Ng, N.L.; Varutbangkul, V.; Flagan, R.C.; Seinfeld, J.H. Gas-phase products and secondary aerosol yields from the photooxidation of 16 different terpenes. *J. Geophys. Res. Atmos.* **2006**, *111*, D17305. [CrossRef]
33. Rollins, A.W.; Kiendler-Scharr, A.; Fry, J.L.; Brauers, T.; Brown, S.S.; Dorn, H.-P.; Dubé, W.P.; Fuchs, H.; Mensah, A.; Mentel, T.F.; et al. Isoprene oxidation by nitrate radical: Alkyl nitrate and secondary organic aerosol yields. *Atmos. Chem. Phys.* **2009**, *9*, 6685–6703. [CrossRef]
34. Slade, J.H.; de Perre, C.; Lee, L.; Shepson, P.B. Nitrate radical oxidation of γ -terpinene: Hydroxy nitrate, total organic nitrate, and secondary organic aerosol yields. *Atmos. Chem. Phys.* **2017**, *17*, 8635–8650. [CrossRef]
35. Fry, J.L.; Brown, S.S.; Middlebrook, A.M.; Edwards, P.M.; Campuzano-Jost, P.; Day, D.A.; Jimenez, J.L.; Allen, H.M.; Ryerson, T.B.; Pollack, I.; et al. Secondary organic aerosol (SOA) yields from NO_3 radical + isoprene based on nighttime aircraft power plant plume transects. *Atmos. Chem. Phys.* **2018**, *18*, 11663–11682. [CrossRef]
36. Ng, N.L.; Kwan, A.J.; Surratt, J.D.; Chan, A.W.H.; Chhabra, P.S.; Sorooshian, A.; Pye, H.O.T.; Crounse, J.D.; Wennberg, P.O.; Flagan, R.C.; et al. Secondary organic aerosol (SOA) formation from reaction of isoprene with nitrate radicals (NO_3). *Atmos. Chem. Phys.* **2008**, *8*, 4117–4140. [CrossRef]
37. Kanakidou, M.; Seinfeld, J.H.; Pandis, S.N.; Barnes, I.; Dentener, F.J.; Facchini, M.C.; Van Dingenen, R.; Ervens, B.; Nenes, A.; Nielsen, C.J.; et al. Organic aerosol and climate modelling: A review. *Atmos. Chem. Phys.* **2005**, *5*, 1053–1123. [CrossRef]
38. IPCC. *Climate Change 2013: The Physical Scientific Basis. Contribution of Working Group I to the Fifth Assessment Report of the Intergovernmental Panel on Climate Change*; Stocker, T.F., Qin, D., Plattner, G.-K., Tignor, M., Allen, S.K., Boschung, J., Nauels, A., Xia, Y., Bex, V., Midgley, P.M., Eds.; Cambridge University Press: Cambridge, UK; New York, NY, USA, 2013; p. 1535.
39. Nel, A. Air pollution-related illness: Effects of particles. *Science* **2005**, *308*, 804–806. [CrossRef]
40. Sharaiwa, M.; Ueda, K.; Pozzer, A.; Lammel, G.; Kampf, C.J.; Fushimi, A.; Enami, S.; Arangio, A.M.; Fröhlich-Nowoisky, J.; Fujitani, Y.; et al. Aerosol Heatlth Effects from Molecular to Global Scales. *Environ. Sci. Technol.* **2017**, *51*, 13545–13567. [CrossRef]
41. Rollins, A.W.; Browne, E.C.; Min, K.-E.; Pusede, S.E.; Wooldridge, P.J.; Gentner, D.R.; Goldstein, A.H.; Liu, S.; Day, D.A.; Russell, L.M.; et al. Evidence for NO_x control over nighttime SOA formation. *Science* **2012**, *337*, 1210–1212. [CrossRef]
42. Kiendler-Scharr, A.; Mensah, A.A.; Friese, E.; Topping, D.; Nemitz, E.; Prevot, A.S.H.; Äijälä, M.; Allan, J.; Canonaco, F.; Canagaratna, M.; et al. Ubiquity of organic nitrates from nighttime chemistry in the European submicron aerosol. *Geophys. Res. Lett.* **2016**, *43*, 7735–7744. [CrossRef]
43. Bohnenstengel, S.I.; Belcher, S.E.; Aiken, A.; Allan, J.D.; Allen, G.; Bacak, A.; Bannan, T.J.; Barlow, J.F.; Beddows, D.C.S.; Bloss, W.J.; et al. Meteorology, Air Quality, and Health in London: The ClearfLo Project. *Bull. Am. Meteorol. Soc.* **2015**, *96*, 779–804. [CrossRef]
44. Bannan, T.J.; Bacak, A.; Muller, J.B.; Booth, A.M.; Jones, B.; Le Breton, M.; Leather, K.E.; Ghalaieny, M.; Xiao, P.; Shallcross, D.E.; et al. Importance of direct anthropogenic emissions of formic acid measured by a chemical ionisation mass spectrometer (CIMS) during the Winter ClearfLo Campaign in London, January 2012. *Atmos. Environ.* **2014**, *83*, 301–310. [CrossRef]
45. Bannan, T.J.; Booth, A.M.; Bacak, A.; Muller, J.B.A.; Leather, K.E.; Le Breton, M.; Jones, B.; Young, D.; Coe, H.; Allan, J.; et al. The first UK measurements of nitryl chloride using a chemical ionisation mass spectrometer in central London in the summer of 2012, and an investigation of the role of Cl atom oxidation. *J. Geophys. Res. Atmos.* **2015**, *120*, 5638–5657. [CrossRef]

46. Bannan, T.J.; Bacak, A.; Le Breton, M.; Flynn, M.; Ouyang, B.; McLeod, M.; Jones, R.; Malkin, T.L.; Whalley, L.K.; Heard, D.E.; et al. Ground and airborne UK measurements of nitryl chloride: An investigation of the role of Cl atom oxidation at Weybourne Atmospheric Observatory. *J. Geophys. Res. Atmos.* **2017**, *122*, 11–154. [CrossRef]
47. Wang, X.; Wang, T.; Yan, C.; Tham, Y.J.; Xue, L.; Xu, Z.; Zha, Q. Large daytime signals of N_2O_5 and NO_3 inferred at 62 amu in a TD-CIMS: Chemical interference or a real atmospheric phenomenon? *Atmos. Meas. Tech.* **2014**, *7*, 1–12. [CrossRef]
48. Le Breton, M.; Bacak, A.; Muller, J.B.A.; Bannan, T.J.; Kennedy, O.; Ouyang, B.; Xiao, P.; Ashfold, M.N.R.; Bauguitte, S.J.-B.; Shallcross, D.E.; et al. The first airborne inter-comparison of N_2O_5 measurements over the UK using a Chemical Ionisation Mass Spectrometer (CIMS) and Broadband Cavity Enhanced Absorption Spectrometer (BBCEAS) during the RONOCO 2010/2011 campaign. *Anal. Meth.* **2014**, *6*, 9731–9743. [CrossRef]
49. Grell, G.A.; Peckham, S.E.; Schmitz, R.; McKeen, S.A.; Frost, G.; Skamarock, W.C.; Eder, B. Fully coupled "online" chemistry within the WRF model. *Atmos. Environ.* **2005**, *39*, 6957–6975. [CrossRef]
50. Dee, D.P.; Uppala, S.M.; Simmons, A.J.; Berrisford, P.; Poli, P.; Kobayashi, S.; Andrae, U.; Balmaseda, M.A.; Balsamo, G.; Bauer, P.; et al. The ERA-interim reanalysis: Configuration and performance of the data assimilation system. *Q. J. R. Meteorol. Soc.* **2011**, *137*, 553–597. [CrossRef]
51. Emmons, L.K.; Walters, S.; Hess, P.G.; Lamarque, J.-F.; Pfizer, G.G.; Fillmore, D.; Granier, C.; Guenther, A.; Kinnison, D.; Laepple, T.; et al. Description and evaluation of the Model for Ozone and Related chemical Tracers, version 4 (MOZART-4). *Geosci. Model. Dev.* **2010**, *3*, 43–67. [CrossRef]
52. Guenther, A.; Karl, T.; Harley, P.; Wiedinmyer, P.; Palmer, P.I.; Geron, C. Estimates of global terrestrial isoprene emissions using MEGAN (Model of Emissions of Gases and Aerosols from Nature). *Atmos. Chem. Phys.* **2006**, *6*, 3181–3210. [CrossRef]
53. Sakulyanontvittaya, T.; Duhl, T.; Wiedinmyer, C.; Helmig, D.; Matsunaga, S.; Potosnak, M.; Milford, J.; Guenther, A. Monoterpene and sesquiterpene emission estimates for the United States. *Environ. Sci. Technol.* **2008**, *42*, 1623–1629. [CrossRef]
54. Kuenen, J.J.P.; Visschedijk, A.J.H.; Jozwicka, M.; Denier van der Gon, H.A.C. TNO-MACC_IIemission inventory; a multi-year (2003–2009) consistent high-resolution European emission inventory for air quality modelling. *Atmos. Chem. Phys.* **2014**, *14*, 10963–10976. [CrossRef]
55. Jenkin, M.E.; Watson, L.A.; Utembe, S.R.; Shallcross, D.E. A Common Representative Intermediates (CRI) mechanism for VOC degradation. Part 1: Gas phase mechanism development. *Atmos. Environ.* **2008**, *42*, 7185–7195. [CrossRef]
56. Watson, L.A.; Shallcross, D.E.; Utembe, S.R.; Jenkin, M.E. A Common Representative Intermediates (CRI) mechanism for VOC degradation. Part 2: Gas phase mechanism reduction. *Atmos. Environ.* **2008**, *42*, 7196–7204. [CrossRef]
57. Wild, O.; Zhu, X.; Prather, M.J. Fast-J: Accurate simulation of IN- and Below-Cloud Photolysis in Tropospheric Chemical Models. *J. Atmos. Chem.* **2000**, *37*, 245–282. [CrossRef]
58. Khan, M.A.H.; Clements, J.; Lowe, D.; McFiggans, G.; Percival, C.J.; Shallcross, D.E. Investigating the behaviour of the CRI-MECH gas-phase chemistry scheme on a regional scale for different seasons using the WRF-Chem model. *Atmos. Res.* **2019**, *229*, 145–156. [CrossRef]
59. Archer-Nicholls, S.; Lowe, D.; Utembe, S.; Allan, J.; Zaveri, R.A.; Fast, J.D.; Hodnebrog, Ø.; van der Gon, H.D.; McFiggans, G. Gaseous chemistry and aerosol mechanism developments for version 3.5.1 of the online regional model, WRF-Chem. *Geosci. Model. Dev.* **2014**, *7*, 2557–2579. [CrossRef]
60. Dörich, R.; Eger, P.; Lelieveld, J.; Crowley, J.N. Iodide CIMS and m/z 62: The detection of HNO_3 as NO_3^- in the presence of PAN, peroxyacetic acid and ozone. *Atmos. Meas. Tech.* **2021**, *14*, 5319–5332. [CrossRef]
61. Liebmann, J.; Karu, E.; Sobanski, N.; Schuladen, J.; Ehn, M.; Schallhart, S.; Quéléver, L.; Hellen, H.; Hakola, H.; Hoffmann, T.; et al. Direct measurement of NO_3 radical reactivity in a boreal forest. *Atmos. Chem. Phys.* **2018**, *18*, 3799–3815. [CrossRef]
62. Liebmann, J.M.; Muller, J.B.A.; Kubistin, D.; Claude, A.; Holla, R.; Plass-Dülmer, C.; Lelieveld, J.; Crowley, J.N. Direct measurements of NO_3 reactivity in and above the boundary layer of a mountaintop site: Identification of reactive trace gases and comparison with OH reactivity. *Atmos. Chem. Phys.* **2018**, *18*, 12045–12059. [CrossRef]
63. Kames, J.; Schurath, U. Alkyl nitrates and bifunctional nitrates of atmospheric interest: Henry's law constants and their temperature dependencies. *J. Atmos. Chem.* **1992**, *15*, 79–95. [CrossRef]
64. Utembe, S.R.; Cooke, M.C.; Archibald, A.T.; Shallcross, D.E.; Derwent, R.G.; Jenkin, M.E. Simulating secondary organic aerosol in a 3-D Lagrangian chemistry transport model using the reduced Common Representative Intermediates mechanism (CRI v2-R5). *Atmos. Environ.* **2011**, *45*, 1604–1614. [CrossRef]
65. Khan, M.A.H.; Jenkin, M.E.; Foulds, A.; Derwent, R.G.; Percival, C.J.; Shallcross, D.E. A modeling study of secondary organic aerosol formation from sesquiterpenes using the STOCHEM global chemistry and transport model. *J. Geophys. Res. Atmos.* **2017**, *122*, 4426–4439. [CrossRef]